Quantum Hall states under conditions of vanishing Zeeman energy

F. J. Teran,[1,2] M. Potemski,[1] D. K. Maude,[1] T. Andrearczyk,[3] J. Jaroszyński,[3,4] T. Wojtowicz,[3] and G. Karczewski[3]
[1]*Laboratoire National des Champs Magnétiques Intenses, CNRS-UJF-UPS-INSA, 38042 Grenoble, France*
[2]*Instituto Madrileño de Estudios Avanzados en Nanociencia, Ciudad Universitaria de Cantoblanco, 28049 Madrid, Spain*
[3]*Institute of Physics, Polish Academy of Sciences, PL-02668 Warsaw, Poland*
[4]*National High Magnetic Field Laboratory, Tallahassee, Florida 32306, USA*
(Received 1 September 2010; published 21 December 2010)

We report on magnetotransport measurements of a two-dimensional electron gas confined in a $Cd_{0.997}Mn_{0.003}Te$ quantum well structure under conditions of vanishing Zeeman energy. The electron Zeeman energy has been tuned via the *s-d* exchange interaction in order to probe different quantum Hall states associated with metallic and insulating phases. We have observed that reducing Zeeman energy to zero does not necessary imply the disappearing of quantum Hall states, i.e., a closing of the spin gap. The spin-gap value under vanishing Zeeman-energy conditions is shown to be dependent on the filling factor. Numerical simulations support a qualitative description of the experimental data presented in terms of a crossing or an avoided crossing of spin split Landau levels with same orbital quantum number *N*.

DOI: 10.1103/PhysRevB.82.245120 PACS number(s): 71.10.Ca, 73.43.−f, 75.50.Pp

I. INTRODUCTION

In a quantizing magnetic field, the physics of a two-dimensional electron gas (2DEG) at very low temperatures is controlled by electron-electron interactions which dominate over the single-particle physics leading to exotic collective ground states.[1,2] For example, the spin exchange energy often dominates over the single-particle Zeeman energy in the fractional and integer quantum Hall regimes.[3–22] The rich physics of the quantum Hall ferromagnetism[1,16] has attracted considerable interest when two spin-split Landau levels with different spin index (σ) and orbital quantum number (N) are brought in coincidence.[4–9] In this case, the quantum Hall effect (QHE) may exhibit hysteretic features with a complicated phenomenology[7,9] related to phase transitions at nonzero temperatures. The behavior under these conditions corresponds to Ising ferromagnetic systems (i.e., with easy-axis anisotropy).[6] Such behavior can be explained in terms of domain walls[6] or distinct symmetry-broken states.[10]

Equally, the crossing of spin-split Landau levels with the same N and different spin index leads to interesting physics.[11,13,14] In this case, QHE exhibits a different phenomenology related to no finite-temperature phase transitions without hysteretic features. The behavior under these conditions corresponds to Heisenberg ferromagnetic systems (i.e., isotropic anisotropy)[6] leading to nonzero electron-spin gaps in the energy spectrum of a 2DEG under conditions of vanishing Zeeman energy. This behavior has been observed in GaAs-based structures in the integer quantum Hall regime at $\nu=1$ and 3. This could be explained as a consequence of the well established model[16–20] of electron-electron exchange interaction (at least for $\nu=1$) which forces a ferromagnetic ordering of the electronic spins at odd filling factors.[11,13,14] Therefore, any small perturbation opens the electron spin gap (Δ_S) even when Zeeman energy is zero. Reasoning in these terms also implies that the exchange contribution to Δ_S always dominates over the Zeeman term. This is in agreement with routine experimental observations in 2DEGs confined in III/V based structures which clearly show that Δ_S deduced from activated transport data at odd filling factors always greatly exceeds the single-particle Zeeman energy.[11,13,14] In addition, electronic spins cannot be treated as an isolated system but unavoidably interact with localized spins of nuclei[23] or localized spins of substitutional magnetic ions, such us Mn^{2+}.[9,24–27] The incorporation of localized magnetic moments in diluted magnetic semiconductors (DMS) offers unique spin splitting engineering[28] via the *s-d* exchange interaction between the electron and magnetic ion spins.[29] This can potentially be exploited to probe the spontaneous ferromagnetic order of a 2DEG via Δ_S when the electron Zeeman energy is continuously tuned through zero.

Here, we report on the study of QHE in a *n*-type modulation doped $Cd_{0.997}Mn_{0.003}Te$ quantum well (QW) structure under conditions of vanishing Zeeman energy. So far, the standard method to tune the electron g factor through zero in semiconductor structures was to apply hydrostatic pressure.[14] However, this method offers rather limited range of tunability of the Zeeman energy and can also modify the carrier density or the mobility. The incorporation of substitutional magnetic moments such as Mn^{2+} in CdTe QW structures offers an additional possibility of tuning the electron spin splitting via the *s-d* exchange interaction between the spins of 2DEG and the localized magnetic moments.[30] In a simple approach, the extended 2D electron and localized Mn^{2+} spins can be treated as two paramagnetic subsystems. Thus, a single electron spin feels the external magnetic field and the mean field resulting from the Mn^{2+} spin polarization. Due to the opposite signs of the bare Zeeman and *s-d* exchange terms in a $Cd_{1-x}Mn_xTe$ QW, the magnetic field dependence of the total-electron Zeeman energy (E_Z) results from the competition between these two contributions. At low magnetic fields where the *s-d* exchange interaction term dominates, E_Z has large and positive values related to the *s-d* exchange term. On increasing the magnetic field, the bare Zeeman term increases linearly whereas the *s-d* exchange interaction term saturates. Therefore, at high magnetic fields E_Z decreases because of the negative contribution related to the bare Zeeman term (see left inset of Fig. 1). Thus, E_Z

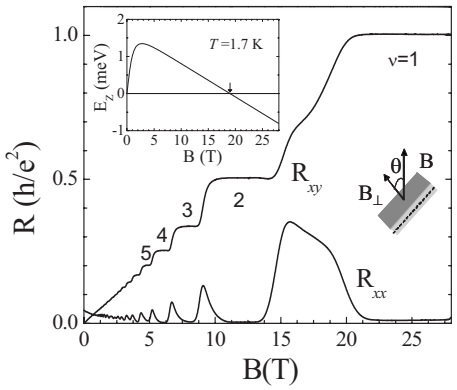

FIG. 1. Magnetic field dependence of R_{xx} and R_{xy} under perpendicular magnetic fields ($\theta=0°$) at $T=1.7$ K in our QW structure. Left inset: Magnetic field dependence of E_Z at $T=1.7$ K calculated according to Eq. (1). The arrow indicates the magnetic field when $E_z=0$. Right inset: schematic indicating sample's orientation to magnetic field.

reaches zero value at a given magnetic field for which Zeeman term is equal to *s-d* exchange term what depends on the Mn concentration. Thus, the particular magnetic field dependence of E_Z in $Cd_{1-x}Mn_xTe$ QW structures allows to study the evolution of a given quantum Hall state when E_Z is continuously tuned from positive to negative values through zero. This can be achieved by simply tilting the plane of the 2D electron sheet with respect to the magnetic field direction. That offers an unique opportunity to probe the ferromagnetic phenomenology of Heisenberg systems when the value of E_Z is modulated and the sign is inverted. The clear advantage of DMS systems is the wide range over which the g factor can be continuously tuned without any changes in the mobility or carrier density. The disadvantage lies in the lower mobility (below 2×10^5 cm^2 V^{-1} s^{-1}) of a 2DEG confined in magnetic QWs (Ref. 31) with respect to their III-V nonmagnetic counterparts. The experimental results presented in this work show that the condition of vanishing effective Zeeman energy in $Cd_{1-x}Mn_xTe$ QWs does not necessarily imply that Δ_S is zero. We also observe that the opening or closing of the Δ_S when $E_Z=0$ tightly depend on the filling factor.

This paper is organized as follows: in Sec. II, we present a description of the sample structure and the experimental procedure. In Sec. III, we show the magnetotransport data obtained from the tilted-field experiments, notably the evolution of longitudinal (R_{xx}) and transversal (R_{xy}) resistances as a function of E_Z and temperature for different filling factors. The R_{xy} shows the development of plateau between $\nu=2$ and 1. This resistance feature is not associated with any quantum Hall state but rather related to the condition $E_Z=0$. Moreover, the evolution of R_{xx} minima as the Zeeman energy passes through zero indicates that Δ_S remains open at $\nu=3$ but closes at $\nu=5$. In addition, the evolution of the R_{xx} maxima on either side of $\nu=3$ (around $\nu=7/2$ and 5/2) under $E_Z=0$ conditions is markedly different, suggesting a different opening of Δ_S. In Sec. IV, we present numerical simulations to qualitatively describe and discuss the Δ_S dependence on E_Z and magnetic fields at distinct filling factors: $\nu=3$ and 5 and $\nu=7/2$, 5/2 and 3/2. Reasoning in terms of the density of states (DOS) at the Fermi level (E_F), we find two different situations which lead to distinct amount of DOS at the Fermi level [DOS(E_F)] under conditions of vanishing Zeeman energy. This depends upon whether the E_F lies inside either the upper or the lower spin level of a given spin-split Landau level. Finally, Sec. V summarizes the important points found in this work.

II. EXPERIMENTAL DETAILS

For the investigation, a *n*-type modulation-doped structure made of a single 10-nm-thick $Cd_{0.997}Mn_{0.003}Te$ QW embedded between $Cd_{0.8}Mg_{0.2}Te$ barriers was employed. The 2DEG is formed by placing iodine doped *n*-type $Cd_{0.8}Mg_{0.2}Te$ layer separated from the $Cd_{0.997}Mn_{0.003}Te$ QW by a 10-nm-thick undoped $Cd_{0.8}Mg_{0.2}Te$ spacer. For the magnetotransport measurements a standard mesa etched Hall bar was defined (typical dimensions 0.5×1 mm) with six electrical contacts to measure the R_{xx} and R_{xy} resistance tensor components. The 2D electron concentration obtained from either the Hall resistance or the periodicity of the Shubnikov de Haas oscillations is $n_e=5.9\times10^{11}$ cm^{-2} and the mobility $\mu_e=6\times10^4$ cm^2 V^{-1} s^{-1} at liquid helium temperatures. The sample was mounted on a rotation stage to tilt the sample with respect to magnetic field direction at temperatures (T) ranging from 4.2 K down to 40 mK and magnetic fields up to 28 T. The sample resistance components were measured using ac techniques (10.7 Hz with electrical currents $\sim$10–100 nA). Whereas E_Z is defined by the total magnetic field (B), the filling factor is determined by the magnetic field component which is perpendicular to the 2D plane ($B_\perp$) (see right inset in Fig. 1). Thus, by rotating the sample the value of E_Z at a given filling factor is varied from positive to negative values passing through zero.

III. MAGNETOTRANSPORT RESULTS

A. Longitudinal and transverse resistance at perpendicular magnetic fields

Figure 1 shows the magnetotransport measurements of our sample under perpendicular magnetic fields up to $B=28$ T at $T=1.7$ K. A well-developed Landau quantization at the integer quantum Hall regime is observed: well-pronounced Shubnikov de Haas oscillations in R_{xx} and quantized plateaus in R_{xy}. The rather broad R_{xy} plateaus associated to low filling factors (for instance, $\nu=1$ and 2) and the low 2DEG mobility reveal the presence of relevant disorder in our sample. At low magnetic fields (where $E_Z\geq\hbar\omega_c$), Shubnikov de Haas oscillations show complex beating patterns which have been discussed in detail in a previous work.[24] At higher magnetic fields (where $\hbar\omega_c>E_Z$), both R_{xx} and R_{xy} show a typical QHE for a spin polarized 2DEG: resistance plateaus and minima associated with a continuous sequence of odd and even integer filling factors. However, certain R_{xx} and R_{xy} irregularities appear in the range of $B=14-22$ T. At these magnetic fields, the R_{xx} maxima between $\nu=2$ and 1 is anomalously distorted so that the development of an additional minimum in R_{xx} could be envisaged

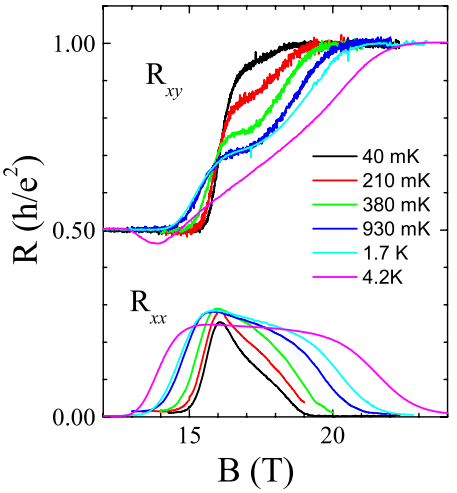

FIG. 2. (Color online) Temperature dependence of R_{xx} and R_{xy} for $\theta=0°$ in the vicinity of $\nu=3/2$.

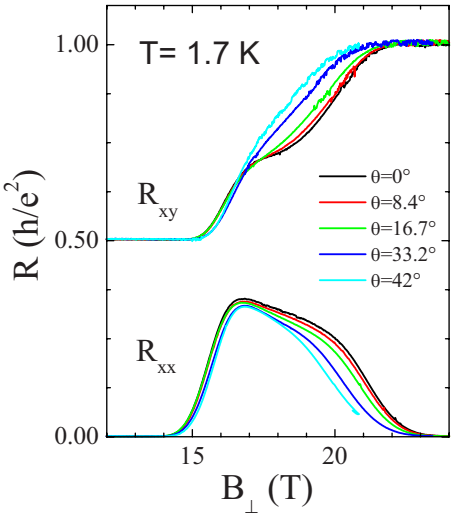

FIG. 3. (Color online) R_{xx} and R_{xy} as a function of perpendicular magnetic fields, $B_\perp$, at $T=1.7$ K for different tilt angles θ in the vicinity of $\nu=3/2$.

around $B=17$ T. In parallel, a kink, resembling the development of quantum Hall plateau, is observed in the R_{xy} trace. These anomalies have been previously related to the appearance of the $\nu=4/3$ fractional quantum Hall state.[32] However, the temperature dependence of R_{xy} and R_{xy}, shown in Fig. 2, rules out such a possibility. While there is some evidence for the existence of a plateau at intermediate temperatures (ranging 210 mK–1.7 K), the feature washes out at the lowest temperatures rather than fully developing as expected for a fractional state. Indeed, the value of the anomalous plateau tightly depends on temperature: whereas at the lowest temperature ($T=40$ mK), the R_{xy} anomalous plateau almost reaches the value of h/e^2, the value drops near to $0.5h/e^2$ at the highest $T=4.2$ K. The nonquantization of the developing plateau is a strong indication that an alternative explanation to fractional states should be sought. Simultaneously, the R_{xx} maxima continuously broadens when increasing temperature. In order to clarify whether the vanishing of E_Z is related to these resistance anomalies, we model the magnetic field and temperature dependence of E_Z in our sample by assuming[29] that

$$E_Z = g_e \mu_B B + E_{s\text{-}d} \mathbb{B}_{5/2}(B,T,T_0), \tag{1}$$

where $g_e=-1.6$ is the electron g factor in CdTe,[33] μ_B is the Bohr magneton, $E_{s\text{-}d}=1.25$ meV is the s-d exchange interaction term between free electron and localized Mn^{2+} determined here from the low magnetic field transport measurements,[24] $\mathbb{B}_{5/2}(B,T,T_0)$ is the modified Brillouin function, and T_0 is the effective temperature of the Mn spin subsystem[29] considering the magnetization correction due to the antiferromagnetic Mn^{2+}-Mn^{2+} interactions. In our particular sample, $T_0=0.12$ K was determined from transport measurements at low magnetic fields.[24] The expected magnetic field dependence of E_Z in our sample at $T=1.7$ K is shown in the inset of Fig. 1. At low magnetic fields, E_Z has large and positive values related to the exchange term. Once the exchange term is saturated, E_Z decreases linearly with magnetic field and crosses zero around $B\sim 19$ T, i.e., in the magnetic field range in which the R_{xx} and R_{xy} anomalies are observed.

In order to probe the relationship between the R_{xy} and R_{xx} anomalies associated to $\nu=3/2$ and the $E_Z=0$ condition, we have performed tilted-field magnetotransport experiments shown in Fig. 3. The resistance anomalies observed at $B_\perp=19$ T weaken when tilting the sample, i.e., when the $E_Z=0$ condition is shifted toward lower $B_\perp$: the R_{xx} high-field shoulder decreases and the R_{xy} nonquantized plateau significantly increases its value. This strongly suggests that those resistance anomalies observed between $B_\perp=14-24$ T are related to the vanishing of E_Z expected in this magnetic field range (see left inset of Fig. 1).

To further elucidate the influence of a vanishing Zeeman energy on the magnetotransport properties, we have investigated the influence of tuning the Zeeman energy on integer quantum Hall states. At integer filling factors and low temperatures, our 2DEG shows zero resistivity and zero conductivity ($\rho_{xx}=\sigma_{xx}=0$) indicating the existence of a well-developed gap. Characteristically for insulating systems, the gap can be determined by thermally activated transport measurements. This procedure yields reliable gap values for clean 2DEG (Ref. 13) (i.e., narrow Landau-level broadening). However, this is not the case for our 2DEG as revealed by the wide R_{xy} plateaus observed in Fig. 1 and the low carrier mobility. Such plateau broadening can be related to the alloy disorder associated with ternary compounds, to the long-range disorder associated with iodine donor impurities and/or with the presence of background dopants in the QW region. In a first approach, all these disorder mechanisms increase Landau-level broadening leading to a large number of localized states. Nevertheless, thermally activated gaps obtained by temperature-dependent measurements in our sample may provide a qualitative evolution of Δ_S when tuning E_Z at given filling factor. Thus, we investigate the evolution of R_{xx} when Zeeman energy vanishes at the insulating-like quantum Hall states $\nu=3$ and 5. Furthermore, we similarly study the evolution of R_{xx} when Zeeman energy

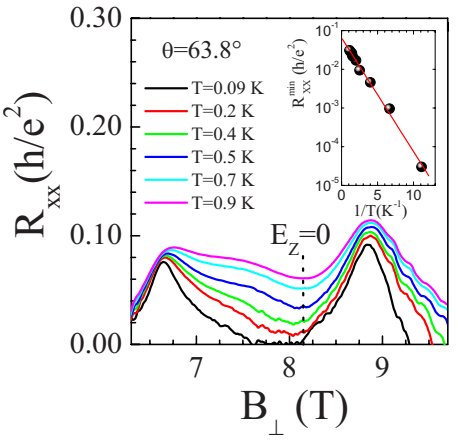

FIG. 4. (Color online) Temperature dependence of R_{xx} minima related to $\nu=3$ for a tilted angle $\theta=63.8°$ for which $E_Z=0$ is expected at $B_{\perp 0}=8.1$ T. Inset: Arrhenius plot of the temperature dependence of R_{xx} at $B_{\perp 0}=8.1$ T.

vanishes at the metalliclike quantum Hall states $\nu=7/2$, 5/2, and 3/2.

B. Spin gaps at $\nu=3$ and 5 versus Zeeman splitting

Figure 4 shows R_{xx} measured in the temperature range between 90 and 900 mK and at a fixed tilted angle $\theta=63.8°$. At this particular angle, vanishing Zeeman energy (i.e., $E_Z=0$) and $\nu=3$ coincide at $B_\perp=8.1$ T. Under this condition, a well-defined R_{xx} minimum is observed, reaching zero value below 200 mK. This clearly indicates that Δ_S at $\nu=3$ remains open even under vanishing Zeeman-energy conditions. Assuming a thermally activated behavior, the measured value of the resistance minima ($R_{xx}^{\min}$) at $\nu=3$ can be described by the following expression:

$$R_{xx}^{\min} = R_0 \exp(-E_A/2kT) \tag{2}$$

a plot of $\ln[R_{xx}(T)]$ versus $1/T$ allows us to deduce an activation energy $E_A=0.25$ meV with the prefactor $R_0=0.1h/e^2$ (see inset of Fig. 4). In case of a dirty 2DEG, E_A should be increased by the width of the region of extended states (Γ_{ext}) in order to obtain a better estimate of the spin gap.[13] Thus, $\Delta_S=E_A+\sqrt{2}\Gamma_{ext}$. Simulations of R_{xx} at low fields were performed to model the magnetotransport measurements for our 2DEG system[24] considering $\Gamma_{ext}=0.2$ meV. This value of Γ_{ext} is in agreement with the value of Landau-level broadening ($\Gamma_{ext}=0.075$ meV) employed in numerical simulations described in Sec. IV. Hence, we obtain a value of $\Delta_S=0.53$ meV at $\nu=3$ under $E_Z=0$ conditions.

Figure 5(a) shows the evolution of R_{xx} when the $E_Z=0$ condition is tuned through $\nu=3$ at a fixed temperature ($T=1.7$ K). At $\theta=0°$, R_{xx} shows a well-developed minima at $\nu=3$ which becomes less pronounced when tilting the sample. At $\theta=63.9°$, the conditions $E_Z=0$ and $\nu=3$ coincide. At that angle, the value of R_{xx} at $\nu=3$ shows a maximum. In contrast, R_{xx} at $\nu=3$ recovers minimum values at larger angles (see data at $\theta=72°$). From Eq. (1), we obtain the expected perpendicular magnetic field ($B_{\perp 0}$) for which $E_Z=0$ at a given angle as indicated in the Fig. 5. As expected,

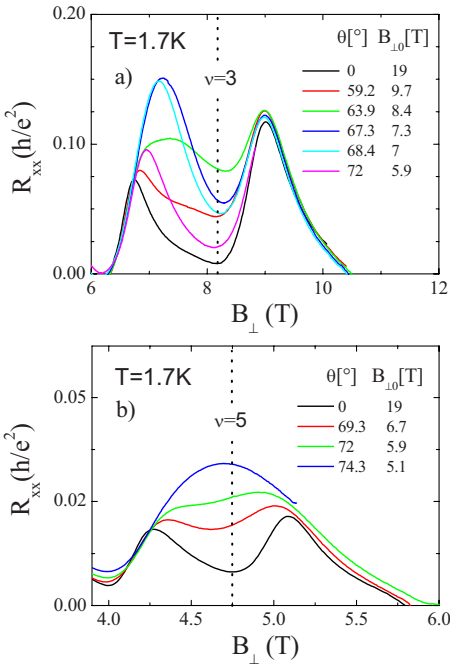

FIG. 5. (Color online) (a) R_{xx} as a function of perpendicular magnetic field $B_\perp$ for different tilt angles θ in the vicinity of $\nu=3$ at $T=1.7$ K. (b) R_{xx} as a function of perpendicular magnetic field $B_\perp$ for different tilt angles θ in the vicinity of $\nu=5$ at $T=1.7$ K. $B_{\perp 0}$ for which $E_Z=0$ is indicated for each angle.

the R_{xx} minimum associated with $\nu=3$ becomes less pronounced as E_Z is initially decreased when the sample is rotated away from the normal configuration. In contrast, the resistance minimum at $\nu=3$ shows its maximum value when $E_Z\approx 0$. Afterwards, the resistance minimum at $\nu=3$ decreases again for large tilt angles when E_Z acquires large and negative values.

The results of similar measurements around $\nu=5$ are quite different [see Fig. 5(b)]. The R_{xx} minimum is transformed into a maximum under vanishing Zeeman-energy conditions. This indicates that, at least for the temperature studied ($T=1.7$ K), Δ_S collapses under conditions of vanishing Zeeman energy. Characteristically, a perfect overlap for the $N=2$ spin-split Landau levels when $E_Z\sim 0$ transforms the R_{xx} minima at $\nu=5$ into a maximum whose amplitude is approximately twice that of the adjacent resistance maxima at $\nu=11/2$ and 9/2. The factor of two can be roughly understood assuming that R_{xx} is proportional to DOS(E_F),[34] which indeed approximately doubles when two spin-split Landau levels overlap. Finally, we have not found any evidence of hysteretic resistance traces around $\nu=3$ and 5 quantum Hall states at the temperature studied ($T=1.7$ K). Assuming a thermally activated behavior from Eq. (1), the measured value of R_{xx} minima at $\nu=3$ for a fixed temperature [Fig. 5(a)] can be used to determine E_A as follows:

$$E_A(E_Z) = 2kT[-\ln(R_{xx}^{\min}) + \ln(R_0)], \tag{3}$$

where $R_0=0.1h/e^2$ obtained from Arrhenius plot under $E_Z=0$ at $\nu=3$ conditions as mentioned above. The value of E_A was determined using Eq. (2), for a large number of angles

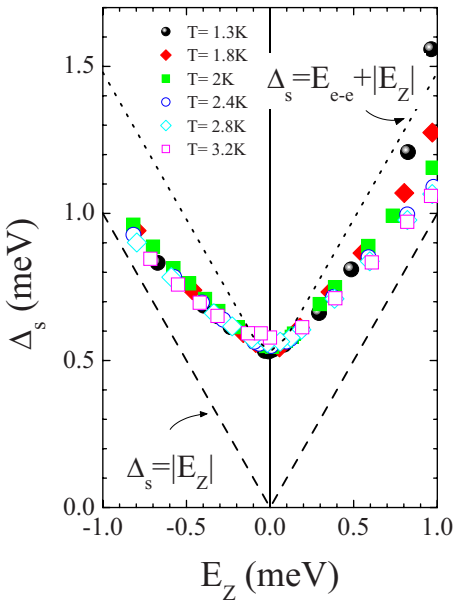

FIG. 6. (Color online) Spin gap as a function of Zeeman energy at $\nu=3$ for different temperatures. Δ_S was obtained by using Eq. (2) as explained in the text. The dotted line represents the spin-gap dependence $\Delta_S=E_Z+E_{e\text{-}e}$ and the dashed line $\Delta_S=E_Z$ as described in the text.

(i.e., different E_Z values at $\nu=3$) and six different temperatures ranging between 1.3 and 3.2 K. Figure 6 shows $\Delta_S(E_A+\sqrt{2\Gamma_{ext}})$ at $\upsilon=3$ as a function of E_Z for different temperatures. The values of Δ_S determined from data taken at different temperatures all collapse onto the same curve which validates our assumption of a thermally activated behavior. As expected, Δ_S has a minimum value, $\Delta_S=0.53$ meV, when $E_Z=0$. This Δ_S value at $E_Z=0$ is in agreement with the one obtained from fitting Eq. (1) shown in the inset of Fig. 4. Such a Δ_S value under vanishing Zeeman-energy conditions seems extremely small in comparison to values of spin gap enhanced by electron-electron interactions. As mentioned above, the large Landau-level broadening associated to this dirty 2DEG may lead to imprecise gap values from thermally activated measurements in the studied temperature range. However, it is enough to provide a qualitative description of the Δ_S dependence on E_Z. The single-particle picture would provide a simple spin-gap dependence with Zeeman energy as being given by $\Delta_S=E_Z$ (see dashed line in Fig. 6). The disagreement of experimental data with this single-particle Δ_S dependence suggests a more complex description. Indeed, $\Delta_S \geq E_Z$ and clearly remains open when $E_Z=0$ at $\nu=3$. Either side of $E_Z=0$, Δ_S increases linearly with E_Z but with different slopes, slightly steeper in the positive E_Z range than in the negative one. Such specific character of the Δ_S slopes may be related to the different behavior of R_{xx} maxima either sides of $\nu=3$ when E_Z is tuned [see Fig. 5(a)]. Inspecting Fig. 6, we notice that $\Delta_S \geq |E_Z|$ when $|E_Z|$ is sufficiently large. On the other hand, $\Delta_S \gg |E_Z|$ only when $E_Z \approx 0$. Reasoning in terms of spin-split Landau levels, such characteristic dependence can be related to the effect of resonant level repulsion. We assign this phenomenon to electron-electron interaction related to electron spin polarization at $\nu=3$. However as mentioned above, it is important to note that the opening of Δ_S in terms of resonant repulsion (avoided crossing) of spin-split $N=1$ Landau levels is not exactly what one would expect from the accepted knowledge of the physics of a 2DEG at odd filling factors in high-quality III-V nanostructures. For a disorder-free 2DEG, we would expect Δ_S to be the sum of the Zeeman energy and the electron-electron exchange energy, $E_{e\text{-}e}$, which is constant for a given filling factor and independent of the Zeeman energy. This would imply that $\Delta_S=E_{e\text{-}e}+|E_Z|$ where $E_{e\text{-}e}$ is the experimental Δ_S value when $E_Z=0$. However, such linear dependence is not reflected in our experimental data (see dotted line in Fig. 6). A model of spin-split Landau-level repulsion (i.e., avoided crossing) is shown to successfully explain our observations at $\nu=3$ as will be described in Sec. IV.

We summarize this section by pointing out the contrasting observation of the avoided crossing of spin-split Landau levels at $\nu=3$ while a crossing of spin-split Landau levels is observed at $\nu=5$.

C. Vanishing Zeeman splitting at half integer filling factors ($\nu=7/2$, 5/2, and 3/2)

We now turn our attention to the behavior of R_{xx} under vanishing Zeeman-energy conditions when E_F lays in the center of a Landau level, i.e., metallic states, at $\nu=7/2$ ($B_\perp \sim 6.6$ T), $\nu=5/2$ ($B_\perp \sim 9$ T), and $\nu=3/2$ ($B_\perp \sim 19$ T). The traces of R_{xx} at $T=1.7$ K and different tilt angles shown in Fig. 5(a) allow us to follow the evolution of the R_{xx} maxima at $\nu=5/2$ and 7/2 when E_Z is tuned through zero in the range +1 to −1 meV. The behavior of the $\nu=5/2$ and 7/2 R_{xx} peaks is significantly different. The position and amplitude of the resistance maximum associated with $\nu=5/2$ remains independent of the effective Zeeman-energy strength. In contrast, R_{xx} maximum associated with $\nu=7/2$ is strongly influenced by E_Z. As E_Z is decreased at $\nu=7/2$ by tilting the sample, the R_{xx} maxima broadens (see data measured at $\theta=59.2°$) on the high magnetic field side and its amplitude increases. At $\theta=67.3°$, $E_Z=0$ and $\nu=7/2$ conditions coincide. In this situation, the amplitude of the R_{xx} maximum related to $\nu=7/2$ is roughly twice the value at $\theta=0°$. At larger tilt angles, E_Z increases (but with a negative sign) leading to the recovery of R_{xx} trace observed at $\theta=0°$. Assuming that R_{xx} is proportional to the DOS(E_F), it is intuitively clear that the doubling of the R_{xx} maximum can be interpreted as a result of a double degeneracy (perfect overlap) of spin-split $N=1$ Landau levels. We consider that the effect of the R_{xx} increase can be seen as a characteristic feature indicating some overlap of the otherwise spin-split $N=1$ Landau levels. An unchanged resistance would correspond to a situation in which the DOS(E_F) remains unchanged and therefore Δ_S remains open, which is the case observed for the $\nu=5/2$ R_{xx} maximum. In terms of our model of "repulsing levels," we deduce that spin-split $N=1$ Landau levels may cross at $\nu=7/2$ while they avoid to cross at $\nu=5/2$. We have found no evidence of hysteretic resistance traces around $\nu=7/2$ and 5/2 quantum Hall states at the temperature range studied.

It is also worth noticing that the shapes of the magnetoresistance components at half integer filling factors are related

to quantum phase transitions between metallic and insulating phases.[35] These transitions are described in terms of the universal scaling theory with well-defined values[36] of the critical exponent κ. Investigations of QHE scaling behavior in similar samples are reported somewhere else.[37] These investigations show that the value of κ at half integer filling factors up to $\nu=17/2$ is $\kappa=0.42$ except under $E_Z=0$ conditions when resistance anomalies are observed. Hence, we can expect that the resistance anomalies at half integer fillings originate from the mixing of spin-split Landau levels under $E_Z=0$ conditions as described in next section.

Turning back to the tilted-field behavior of the R_{xx} peak around $\nu=3/2$, we note that this case is a mixing of the $\nu=5/2$ and 7/2 cases. As shown in Fig. 3, the amplitude of the R_{xx} peak observed around $\nu=3/2$ is essentially not affected by tilting the sample as in case of $\nu=5/2$. In contrast, the high-field side of R_{xx} peak narrows when tilting the sample as shown for $\nu=7/2$ large angles ($\theta>67.3°$) where E_Z increases. Simultaneously, the R_{xy} plateau disappears. This particular behavior can be interpreted as the result of a slight overlap between the spin-split $N=0$ Landau levels at $B_\perp \sim 19$ T which diminishes by tilting the sample (i.e., increasing E_Z). The slight overlap can be interpreted as a sign of an avoided crossing of spin-split $N=0$ Landau levels under vanishing Zeeman-energy conditions. Numerical simulations presented in Sec. IV will qualitatively support this interpretation.

We summarize this section by pointing out the observation of the avoided crossing of spin-split Landau levels at $\nu=5/2$ and 3/2 in contrast with the observed crossing of spin Landau levels at $\nu=7/2$.

IV. NUMERICAL SIMULATIONS

In order to qualitatively account the directly visible consequences of different Δ_S values on the magnetotransport properties of the 2DEG, we have performed numerical calculations. In the following section, we develop a simple model which phenomenologically introduces the spin splitting in terms of an energy of interaction for the avoided crossing of the spin-split Landau levels. The model is capable of qualitatively reproducing the experimental data and gives some insight into the evolution of Δ_S with E_Z and filling factor. In order to do that, we assume different interaction terms depending on filling factor. In addition, we assume that the total density of the electronic states under magnetic field can be described by a set of Gaussian broadened Landau levels shown in Fig. 7. The energy of an electron under quantizing magnetic fields which interacts with Mn^{2+} ions within a single-particle picture is given by

$$E_{N,\sigma} = (N + 1/2)\hbar\omega_c + E_Z\sigma, \tag{4}$$

where $N=0,1,2,\ldots$ corresponds to the Landau-level index, σ denotes the electron angular momentum whose z component has the value $+1/2(-1/2)$ for spin up (down), $\hbar\omega_c = eB_\perp/m_e^*$ denotes the cyclotron energy and $m_e^*=0.107m_o$ is the electron effective mass determined by cyclotron resonance.[38] E_Z is given by Eq. (1). In addition, the DOS_{LL} of spin-resolved Landau levels with Gaussian broadening is described by

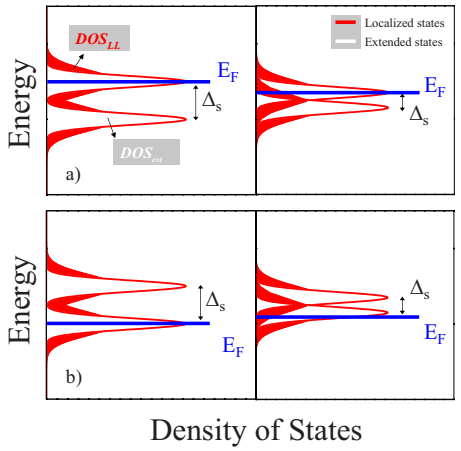

FIG. 7. (Color online) Schematic illustration of the Gaussian DOS_{LL} and DOS_{ext} with widths Γ_{LL} and Γ_{ext}, respectively, in two different conditions of spin-split N Landau-level mixing (right side: mixing, left side: no mixing) when E_F lies (a) in the spin-up N Landau level (as in case of $\nu=3/2$ and 7/2) and (b) in the spin-down N Landau level (as in case of $\nu=5/2$).

$$\mathrm{DOS}_{LL} = \Sigma_{N,\sigma}\frac{eB}{h}\frac{1}{\Gamma_{LL}\sqrt{2\pi}}\exp\left[-\frac{(E-E_{N,\sigma})^2}{2\Gamma_{LL}^2}\right], \tag{5}$$

where Γ_{LL} is the Landau-level Gaussian broadening parameter. We neglect the effective thermal distribution when calculating E_F assuming $T=0$ K for electrons. The procedure of calculating R_{xx} and R_{xy} distinguishes between localized and extended states[34] as shown in Fig. 7. The calculation procedure considers that only the latter ones contribute to the conductivity. In order to do that, we assume that in the central part of each Landau level there exists a band of extended states of Gaussian form whose DOS_{ext} is given by

$$\mathrm{DOS}_{\mathrm{ext}} = \Sigma_{N,\sigma}\frac{eB}{h}\frac{1}{\Gamma_{ext}\sqrt{2\pi}}\exp\left[-\frac{(E-E_{N\uparrow\downarrow})^2}{2\Gamma_{ext}^2}\right], \tag{6}$$

where Γ_{ext} is the extended state Gaussian broadening parameter which is $\Gamma_{ext}<\Gamma_{LL}$. For a given perpendicular magnetic field, E_F is calculated numerically by integrating over the total density of states[34] (i.e., DOS_{LL}). R_{xx} is then taken to be proportional to the density of extended states at E_F, i.e., $DOS_{ext}(E_F)$ and R_{xy} is proportional to the integral of R_{xx}.[34] Our experimental data show that the spin gap remains open even under vanishing E_Z conditions. In order to reproduce such a behavior, we assume that spin-split Landau levels with index N, $E_{N\uparrow,\downarrow}$, are replaced by interacting levels $E^*_{N+,-}$ to calculate DOS_{LL}, DOS_{ext} and E_F. The energy levels $E^*_{N+,-}$ for $N=0$ are given by

$$E^*_{0+,-} = \frac{1}{2}(E_{0\uparrow} - E_{0\downarrow}) \pm \left\{\frac{1}{4}(E_{0\uparrow} - E_{0\downarrow})^2 + \left(\frac{\Delta_0}{2}\right)^2\right\}^{1/2}, \tag{7}$$

where $\Delta_0/2$ is the energy of interaction for the avoided crossing. Physically, Δ_0 corresponds to the experimentally observed spin gap Δ_S under vanishing Zeeman-energy conditions (i.e., when $E_Z=0$).

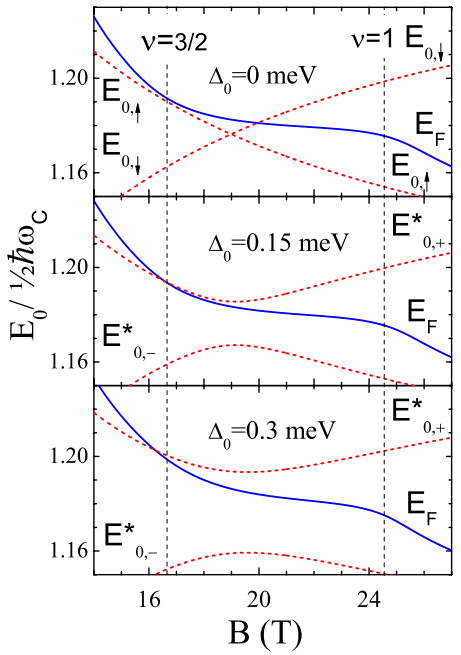

FIG. 8. (Color online) Calculated E_F (solid line) and energy of the spin-split $N=0$ Landau levels normalized to $1/2\hbar\omega_c$ (dotted lines) as a function of magnetic field for $\theta=0°$ and different values of Δ_0 and $T=1.7$ K according to Eq. (7).

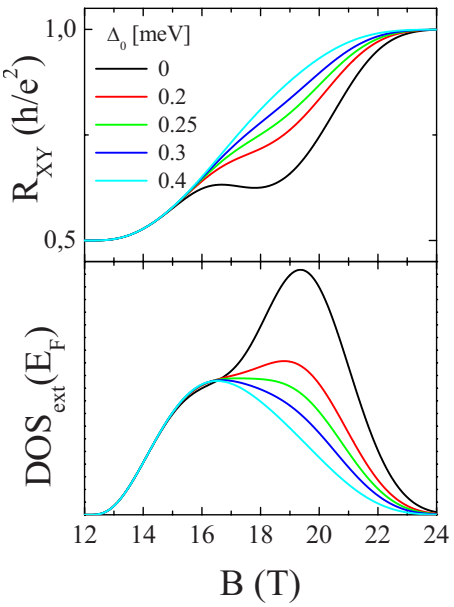

FIG. 9. (Color online) Calculated R_{xy} and $\mathrm{DOS}_{ext}(E_F)$ as a function of magnetic field for $\theta=0°$ and different values of Δ_0 and $T=1.7$ K.

The adjustable parameters in our simulations are: Γ_{LL}, Γ_{ext} and the interaction parameter Δ_0. We have found that our data are best described when $\Gamma_{LL}=0.15$ meV and $\Gamma_{ext}=0.075$ meV both assumed to be constant in the magnetic field range considered ($B=4-28$ T). The value of Γ_{LL} corresponds to a scattering time $\tau=2.75\times10^{-11}$ s in reasonable agreement with the transport scattering time $\tau_t\approx3.65\times10^{-11}$ s deduced from the sample mobility. On the other hand, the interaction parameter Δ_0 was found to be dependent on magnetic field as described below.

A. Vanishing spin gaps at half-integer filling factors ($\nu=7/2$, 5/2, and 3/2)

Initially, we focus our attention on modeling the resistance anomalies observed near $B\sim19$ T at $\nu=3/2$ (see Fig. 2). The nonquantized R_{xy} plateau and the high-field shoulder of R_{xx} can be understood due to the floating up of E_F when the spin split $N=0$ Landau levels approach under vanishing Zeeman-energy conditions. That determines the $\mathrm{DOS}_{ext}(E_F)$ and therefore the resistance components of our system. The position of E_F highly depends on the value of Δ_0 as can be seen in Fig. 8. There, we represent traces of the calculated evolution the spin-split $N=0$ Landau levels and E_F as a function of magnetic field for different values of Δ_0 and $T=1.7$ K (required to calculate E_Z). When $\Delta_0=0$ meV, the spin-split $N=0$ Landau levels cross at $B\sim19$ T. Then, E_F goes slightly above the crossing of spin-split $N=0$ Landau levels leading to an additional peak of the $\mathrm{DOS}_{ext}(E_F)$ and a pronounced broadening as shown in Fig. 9; at the same time a kink appears in R_{xy} which resembles a plateau development (see in Fig. 9). When increasing the value of $\Delta_0=0.2$ meV, the $\mathrm{DOS}_{ext}(E_F)$ reduces due to the fact E_F goes through the center of the upper spin branch Landau level (see Fig. 8) over a wide range of magnetic fields. The positioning of E_F with respect to spin-split Landau levels gives rise to broad and pronounced $\mathrm{DOS}_{ext}(E_F)$ peak around $B=19$ T but with a smaller amplitude than in case of $\Delta_0=0$ meV. Simultaneously, the R_{xy} kink increases its resistance value around $B\sim19$ T but becomes less pronounced with respect to $\Delta_0=0$ meV (see Fig. 9). In contrast, for Δ_0 values ranging 0.25–0.4 meV, the spin split $N=0$ Landau levels have a more pronounced energy distance leading to a significant reduction in $\mathrm{DOS}_{ext}(E_F)$ when E_F goes across the Δ_0 gap (i.e. between $E_{0,+}$ and $E_{0,-}$). The increase of magnetic field raises the degeneracy of the Landau levels pulling down E_F with respect to the center of the upper spin branch (see Fig. 8). This is reflected in the transport properties as a transformation of the $\mathrm{DOS}_{ext}(E_F)$ peak into a high-field shoulder which becomes less pronounced as Δ_0 increases (see Fig. 9). Simultaneously, the R_{xy} kink continuously increases its resistance value and become less pronounced when increasing Δ_0 (see Fig. 9).

In addition, the effect of tilting the sample can be reasonably modeled for $\nu=3/2$ by considering the case of $\Delta_0=0.3$ meV. As shown in Fig. 10, the simulation qualitatively reproduces our observations fairly well (compare with Fig. 3): the value of the R_{xy} plateau increases when tilting the sample, reaching the value of the adjacent integer quantum Hall plateau (i.e., h/e^2) for $\theta>33°$. At this tilt angle, the R_{xy} trace shows an unique slope while for smaller angles two different slopes can be appreciated, in good agreement with the experimental data (see Fig. 3). Simultaneously, the R_{xx} maximum become narrower from the high-field side when tilting the sample, in good agreement with experiments. In our simulations, the behavior of E_F depends on a single parameter which is the ratio of the interaction energy to the Landau-level broadening (Δ_0/Γ_{LL}) so that the determined

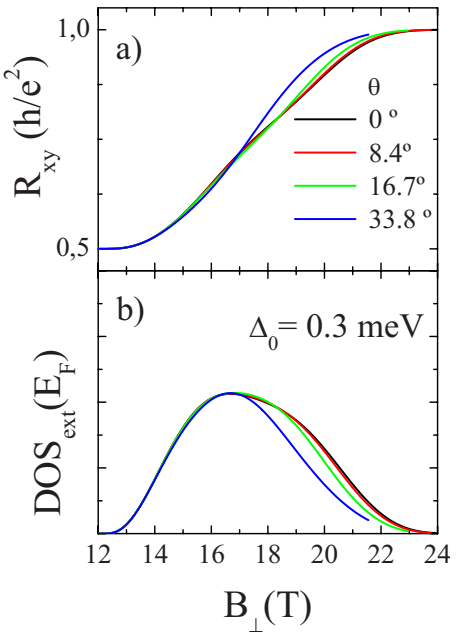

FIG. 10. (Color online) Calculated R_{xy} and $\mathrm{DOS}_{ext}(E_F)$ as a function of perpendicular magnetic field for different tilt angles in the vicinity of $\nu=3/2$ for $\Delta_0=0.3$ meV and $T=1.7$ K.

value of Δ_0 depends on the Landau-level broadening used. This probes that only when electron-electron interaction overcomes disorder at a finite temperature, thermally activated process across a spin gap are observed on the magnetotransport. Another important limitation of the model corresponds to the description of the temperature dependence of the plateau. In a first approach, we may expect that increasing temperature the number of localized states should decrease.[39] This may therefore affect the simulation of Rxy plateau formation and also the broadening of the R_{xx} minima associated with $\nu=1$ shown in Fig. 2. In our calculations, changing Δ_0 should lead to similar effects but it is not the case (see Fig. 9).

Our model qualitatively describes the R_{xy} anomaly associated with $\nu=3/2$ as the result of mixing of localized and extended states at the E_F under vanishing Zeeman-energy conditions. In the standard picture of the integer QHE, the quantization of Hall plateaus is assigned to electron localization and/or to an energy gap [i.e., zero $\mathrm{DOS}(E_F)$]. Moving away from integer filling factors, the $\mathrm{DOS}(E_F)$ and their localization length increases. Hence, free electrons become delocalized leading to the increase of R_{xy} and therefore, the plateau quantization is lost. In our particular case, the mixing of localized-delocalized states at the Fermi level when $E_Z=0$ (see Fig. 7) originates that a given moment E_F leaves extended states to sit in localized states. This leads to the reentrant of an insulating phase earlier than expected and responsible of the observation of a nonquantized plateau. Thus, we can expect a nonquantized plateau when spin-split Landau levels cross under vanishing Zeeman-energy conditions. As shown in Fig. 9, the development degree of the R_{xy} plateau under $E_Z=0$ conditions depends on the value of Δ_0. This term is related to electron-electron interaction and involves thermally activated process. Both mechanisms finally determine the R_{xy} shape at given temperature as shown in Fig. 2. Reasoning in similar terms, this model also explains the appearance of the R_{xx} high-field shoulder at $\nu=3/2$. The success of our qualitative model represents an important goal allowing to predict the appearance of nonquantized plateaus when Landau-level crossing and E_F coincide. The important parameters which favor the observation of such resistance anomalies are Δ_0 and Γ_{LL}. The disorder favors the observations of such resistance phenomena: high magnetic field R_{xx} shoulder (instead of well pronounced peaks) and well developed nonquantized R_{xy} plateau (instead of delta-functionlike plateau reductions[10]). Moreover, our observations reveal that, at the temperature range studied, the crossing (or avoided crossing) of Landau levels with the same N and different σ index does not lead to hysteretic resistance behavior, contrary to the case with different N and σ indexes.[9,10]

Although we conclude in Sec. III C that spin-split Landau levels avoid to cross in both the $\nu=3/2$ and $\nu=5/2$ case, the corresponding R_{xx} resistance maxima behave quite differently when E_Z is continuously varied: the high-field shoulder at $\nu=3/2$ disappears and no changes are observed at $\nu=5/2$. We think, this "asymmetry" results from the fact that partial overlap of spin-split Landau levels affects the position of E_F in a different way depending on whether E_F is located in the vicinity of the upper or of the lower spin level. Our reasoning is schematically illustrated in Fig. 7. The situation when E_F is in the vicinity of the upper spin level, which, for example, corresponds to the case of a 2DEG at $\nu=3/2$, is considered in Fig. 7(a). In Fig. 7(b), E_F lays in the vicinity of the lower spin level which, for example, illustrates the $\nu=5/2$ case. In the left-side panel of Fig. 7 we consider well-separated spin levels and the condition at which the maximum in the R_{xx} should occur (E_F located exactly at the center of the corresponding Landau level). Let us now imagine that we increase the magnetic field but at the same time the spin levels approach leading to a partial overlap. The primary effect of the increase in the magnetic field is to increase the Landau-level degeneracy and therefore to lower E_F with respect to the center of the corresponding spin-split Landau level. This simply translates into a decrease in the corresponding resistance by assuming that $R_{xx}\sim\mathrm{DOS}(E_F)$. However, as shown in Fig. 7, the position of E_F (with respect to the center of the corresponding spin-split Landau level) is also affected by the increasing overlap of the spin levels. We note that the Landau level overlap leads to the decrease in DOS_{ext} available below the center of the upper spin level and to the increase in DOS_{ext} below the center of the lower level. Therefore, by increasing the overlap between spin levels we push E_F up when it is in the vicinity of the upper spin level and push it down when E_F is in the vicinity of the lower spin branch. We expect that the additional "overlap-induced" downward shift of E_F may somehow speed up the decay of the corresponding R_{xx} peak, but the effect of "overlap-induced upward shift" of E_F may have much more pronounced consequences on the observed shape of the corresponding R_{xx} maxima.

Therefore, we may qualitatively understand the effect of the broadening of the $\nu=3/2$ resistance maximum observed on the high-field side when separation between spin-split Landau levels becomes small. Even more severe distortions

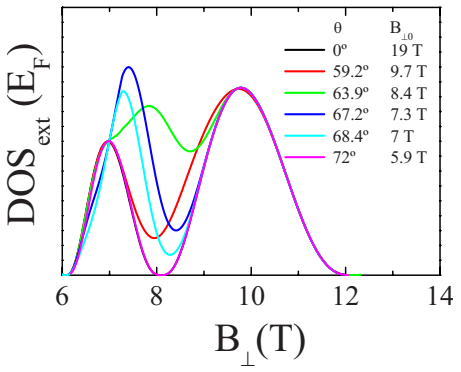

FIG. 11. (Color online) Calculated $DOS_{ext}(E_F)$ as a function of perpendicular magnetic field for different tilt angles in the vicinity of $\nu=3$ considering $\Delta_0=f(B_\perp)$ and $T=1.7$ K as described in the text. $B_{\perp 0}$ is noted for each angle.

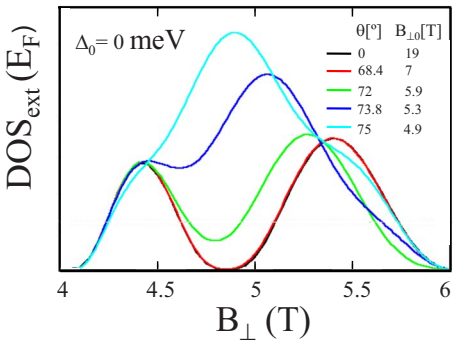

FIG. 12. (Color online) Calculated $DOS_{ext}(E_F)$ as a function of perpendicular magnetic field for different tile angles in the vicinity of $\nu=5$ considering $\Delta_0=0$ meV and $T=1.7$ K as described in the text. $B_{\perp 0}$ is noted for each plot.

of this resistance peak could be expected, for example, the situation when E_F crosses twice the center of the same spin level and therefore the observation of the splitting of the $\nu=3/2$ peak should be, in principle, possible. We show in the next section that our qualitative considerations are confirmed by a more quantitative approach to simulate numerically our experimental results.

B. Spin gaps at $\nu=3$ and 5 versus Zeeman splitting

We now turn to the discussion of the shape of the R_{xx} traces obtained as the effective Zeeman energy is swept through zero in the range $4<\nu<2$ shown in Fig. 5(a). We know that the gap at $\nu=3$ and $\nu=5/2$ remains open with a $\Delta_0=0.3$ meV. The doubling of the resistance peak at $\nu=7/2$ under conditions of vanishing Zeeman energy suggests that Δ_S closes (i.e., $\Delta_0 \ll \Gamma_{LL}$). It is clear that there is a strong filling factor dependence of Δ_0 which rapidly changes from zero to finite values. A rapid opening of Δ_S is well known in GaAs-based 2DEGs and is generally explained in terms of the exchange energy which is proportional to the characteristic Coulomb energy and proportional to the spin polarization of the system.[22] Since, for broadened Landau levels, the spin polarization depends on the size of Δ_S a positive feedback occurs and the onset of spin splitting is generally very abrupt. This can be modeled but requires that the gap and spin polarization be calculated self-consistently. We make the simplistic approximation that the residual gap depends only on the Coulomb energy so that $\Delta_0 \propto \sqrt{B}$. The calculated $DOS_{ext}(E_F)$ as a function of perpendicular magnetic field for different tilt angles and $T=1.7$ K (required to calculate E_Z) are shown in Fig. 11. Given the simplicity of the model used the agreement with the measured resistance [see Fig. 5(a)] is reasonably good. As E_Z passes through zero the peak around $\nu \approx 7/2$ increases in amplitude and shifts to higher fields. To complete our simulations, we consider R_{xx} around $\nu=5$ and show that it is possible to roughly reproduce the experimental results [see Fig. 5(b)]. Assuming $\Delta_0=0$ and $T=1.7$ K, our numerical simulations support the qualitative description of the experimental data concluding that spin-split Landau levels cross (i.e., perfect spin-split Landau-level overlap) when $E_Z=0$ leading to R_{xx} maxima, as shown in Fig. 12.

V. SUMMARY

We have studied the evolution of quantum Hall states under conditions of vanishing Zeeman energy for a 2DEG confined in a $Cd_{0.997}Mn_{0.003}Te$ QW structure. The experimental results presented here show that the condition of vanishing effective Zeeman energy does not necessarily imply the closing of the spin gap. We observe that the opening or closing of the spin gap is a function of the filling factor. Thus, Δ_S remains closed for $\nu=5$ and 7/2 and opened for $\nu=3$, 5/2, and 3/2 at the temperature range studied ($T=1.7$ K). Moreover, the experimental procedure allows the investigation of quantum Hall states under vanishing Zeeman-energy conditions not only for insulating quantum Hall states (i.e., $\nu=3$ and 5) but also for metallic states in the vicinity of $\nu=3/2$, 5/2, and 7/2. A phenomenological model based on an avoided crossing between the two spin-split components of the corresponding Landau level qualitatively reproduce the R_{xx} and R_{xy} measurements at different conditions. Thus, we show that the mixing of localized and extended states under avoided Landau-level crossing conditions leads to the appearance of a nonquantized plateau in the R_{xy}. Our observations can be explained assuming that Δ_S evolves in terms of e-e interactions mediated by disorder leading to a different filling factor dependence.

ACKNOWLEDGMENTS

This work has been supported by the Foundation for Polish Science through subsidy 12/2007, the European Union through the EuroMagNET Contract No. 228043, and the Innovative Economy under Grant No. POIG.01.01.02-00-008/08 related to the European Regional Development Fund.

[1] *Perspectives in Quantum Hall effects*, edited by S. D. Sarma and A. Pinczuk (Wiley, New York, 1997).
[2] A. H. Castro Neto, F. Guinea, N. M. R. Peres, K. S. Novoselov, and A. K. Geim, Rev. Mod. Phys. B **81**, 109 (2009).
[3] H. Cho, J. B. Young, W. Kang, K. L. Campman, A. C. Gossard, M. Bichler, and W. Wegscheider, Phys. Rev. Lett. **81**, 2522 (1998).
[4] R. J. Nicholas, R. J. Haug, K. v. Klitzing, and G. Weimann, Phys. Rev. B **37**, 1294 (1988).
[5] S. Koch, R. J. Haug, K. v. Klitzing, and M. Razeghi, Phys. Rev. B **47**, 4048 (1993).
[6] T. Jungwirth and A. H. MacDonald, Phys. Rev. B **63**, 035305 (2000).
[7] E. P. De Poortere, E. Tutuc, S. J. Papadakis, and M. Shayegan, Science **290**, 1546 (2000).
[8] W. Desrat, F. Giazotto, V. Pellegrini, M. Governale, F. Beltram, F. Capotondi, G. Biasiol, and L. Sorba, Phys. Rev. B **71**, 153314 (2005).
[9] J. Jaroszyński, T. Andrearczyk, G. Karczewski, J. Wróbel, T. Wojtowicz, E. Papis, E. Kamińska, A. Piotrowska, D. Popovic, and T. Dietl, Phys. Rev. Lett. **89**, 266802 (2002).
[10] H. J. P. Freire and J. C. Egues, Phys. Rev. Lett. **99**, 026801 (2007).
[11] A. Usher, R. J. Nicholas, J. J. Harris, and C. T. Foxon, Phys. Rev. B **41**, 1129 (1990).
[12] A. Schmeller, J. P. Eisenstein, L. N. Pfeiffer, and K. W. West, Phys. Rev. Lett. **75**, 4290 (1995).
[13] D. R. Leadley, R. J. Nicholas, J. J. Harris, and C. T. Foxon, Phys. Rev. B **58**, 13036 (1998).
[14] D. K. Maude, M. Potemski, J. C. Portal, M. Henini, L. Eaves, G. Hill, and M. A. Pate, Phys. Rev. Lett. **77**, 4604 (1996).
[15] S. A. J. Wiegers, M. Specht, L. P. Levy, M. Y. Simmons, D. A. Ritchie, A. Cavanna, B. Etienne, G. Martinez, and P. Wyder, Phys. Rev. Lett. **79**, 3238 (1997).
[16] S. M. Girvin, Phys. Today **53**(6), 39 (2000).
[17] C. Kallin and B. I. Halperin, Phys. Rev. B **31**, 3635 (1985).
[18] Yu. A. Bychkov, S. V. Iordanskii, and G. M. Eliashberg, JETP Lett. **33**, 152 (1981).
[19] H. A. Fertig, L. Brey, R. Coté, and A. H. MacDonald, Phys. Rev. B **50**, 11018 (1994).
[20] D. Fukuoka, K. Oto, K. Muro, Y. Hirayama, and N. Kumada, Phys. Rev. Lett. **105**, 126802 (2010).
[21] T. Jungwirth, S. P. Shukla, L. Smrčka, M. Shayegan, and A. H. MacDonald, Phys. Rev. Lett. **81**, 2328 (1998).
[22] J. Kunc, K. Kowalik, F. J. Teran, P. Plochocka, B. A. Piot, D. K. Maude, M. Potemski, V. Kolkovsky, G. Karczewski, and T. Wojtowicz, Phys. Rev. B **82**, 115438 (2010).
[23] S. E. Barrett, G. Dabbagh, L. N. Pfeiffer, K. W. West, and R. Tycko, Phys. Rev. Lett. **74**, 5112 (1995).
[24] F. J. Teran, M. Potemski, D. K. Maude, T. Andrearczyk, J. Jaroszyński, and G. Karczewski, Phys. Rev. Lett. **88**, 186803 (2002).
[25] R. Knobel, N. Samarth, J. G. E. Harris, and D. D. Awschalom, Phys. Rev. B **65**, 235327 (2002).
[26] H. Buhmann, E. G. Novik, V. Daumer, J. Liu, Y. S. Gui, C. R. Becker, and L. W. Molenkamp, Appl. Phys. Lett. **86**, 212104 (2005).
[27] Y. S. Gui, C. R. Becker, J. Liu, V. Daumer, V. Hock, H. Buhmann, and L. W. Molenkamp, Europhys. Lett. **65**, 393 (2004).
[28] T. Wojtowicz *et al.*, J. Cryst. Growth **214-215**, 378 (2000).
[29] J. K. Furdyna, J. Appl. Phys. **64**, R29 (1988).
[30] F. J. Teran, M. Potemski, D. K. Maude, Z. Wilamowski, A. K. Hassan, D. Plantier, J. Jaroszyński, T. Wojtowicz, and G. Karczewski, Physica E **17**, 335 (2003).
[31] V. Kolkovsky, M. Wiater, G. Karczewski, C. Betthausen, A. Vogl, D. Weiss, and T. Wojtowicz, Proceedings of Fifth International School and Conference on Spintronics and Quantum Information Technology, 7–11 July, Krakow, Poland, 2009, p. 77.
[32] F. J. Teran, M. Potemski, D. Maude, T. Andrearczyk, J. Jaroszyński, and G. Karczewski, in *Proceedings of the 25th International Conference on Physics of Semiconductors*, edited by N. Miura and T. Ando (Word Scientific, Singapore/Springer-Verlag, Heidelberg, 2001), Vol. 2, p. 943.
[33] A. A. Sirenko, T. Ruf, M. Cardona, D. R. Yakovlev, W. Ossau, A. Waag, and G. Landwehr, Phys. Rev. B **56**, 2114 (1997).
[34] M. van der Burgt, V. C. Karavolas, F. M. Peeters, J. Singleton, R. J. Nicholas, F. Herlach, J. J. Harris, M. Van Hove, and G. Borghs, Phys. Rev. B **52**, 12218 (1995).
[35] S. L. Sondhi, S. M. Girvin, J. P. Carini, and D. Shahar, Rev. Mod. Phys. **69**, 315 (1997).
[36] W. Li, G. A. Csáthy, D. C. Tsui, L. N. Pfeiffer, and K. W. West, Phys. Rev. Lett. **94**, 206807 (2005).
[37] J. Jaroszyński *et al.*, Physica E **6**, 790 (2000).
[38] M. L. Sadowski, F. J. Teran, M. Potemski, G. Karczewski, M. Kutrowski, J. Jaroszyński, and T. Wojtowicz, in *Proceedings of the 24th International Conference on Physics of Semiconductors*, edited by D. Gershoni (World Scientific, Singapore, 1999).
[39] L. B. Rigal, D. K. Maude, M. Potemski, J. C. Portal, L. Eaves, Z. R. Wasilewski, G. Hill, and M. A. Pate, Phys. Rev. Lett. **82**, 1249 (1999).